

Internal structures of the baryons $\Xi(2030)$ and $\Xi(2120)$

Hao Hei and Yin Huang^{*}*School of Physical Science and Technology, Southwest Jiaotong University, Chengdu 610031, China*

(Received 21 October 2023; accepted 10 January 2024; published 31 January 2024)

Currently, there is much controversy surrounding the interpretation of the $\Xi(2030)$ and $\Xi(2120)$ as traditional hadrons containing double strange quarks. In particular, the ratios of the partial decay widths into $\Lambda\bar{K}$ and $\Sigma\bar{K}$ for $\Xi(2030)$ cannot obtain a suitable explanation under the qss three-quark structure. Thus, we suggest the $\Xi(2030)$ and $\Xi(2120)$ to be $VB(= \bar{K}^*\Sigma/\rho\Xi/\bar{K}^*\Lambda/\phi\Xi/\omega\Xi)$ molecular states. In this work, we perform a systematical investigation of possible molecular states from the $VB(= \bar{K}^*\Sigma/\rho\Xi/\bar{K}^*\Lambda/\phi\Xi/\omega\Xi)$ interaction. The interaction of the system considered is described by the t -channel vector $(\rho, \omega, \phi, \bar{K}^*)$ and pseudoscalar $(\pi, \eta^{(\prime)}, \bar{K})$ meson exchanges. By solving the nonrelativistic Schrödinger equation with the obtained one-boson-exchange potentials, the $VB(= \bar{K}^*\Sigma/\rho\Xi/\bar{K}^*\Lambda/\phi\Xi/\omega\Xi)$ bound states with different quantum numbers are searched. The calculation suggests that $\Xi(2030)$ can be assigned as a P -wave $\bar{K}^*\Sigma/\rho\Xi/\bar{K}^*\Lambda/\phi\Xi/\omega\Xi$ molecular state with spin-parity $J^P = 5/2^+$. The calculation also predicts the existence of four $\bar{K}^*\Sigma/\rho\Xi/\bar{K}^*\Lambda/\phi\Xi/\omega\Xi$ bound states with $J^P = 1/2^\pm$ and $J^P = 3/2^\pm$. The $\Xi(2120)$ may be a candidate for one of these four bound states. If $\Xi(2120)$ is an S -wave molecular state with $J^P = 1/2^-$ or $J^P = 3/2^-$, we suggest determining its spin and parity by studying its decay width, owing to the difference in their molecular components.

DOI: [10.1103/PhysRevD.109.016029](https://doi.org/10.1103/PhysRevD.109.016029)

I. INTRODUCTION

Thanks to significant progress in experiments over the past few decades, researchers have discovered numerous new hadrons [1]. While some of these hadrons exhibit a straightforward quark-antiquark configuration for mesons or a three-quark configuration for baryons [2,3], many states possess enigmatic structures that defy conventional quark-state understanding. These exotic states are often considered to be hadron-hadron molecules, opening the door for the exploration of structural hadrons.

The pursuit of possible hadron-hadron molecular structures represents a pivotal aspect of hadron spectroscopy, offering insights into the mechanisms governing quark dynamics and baryon formation. The deuteron, a well-known bound state comprising neutron-proton components, serves as an early example. Assuming that $\Lambda(1405)$ is a bound state of $\bar{K}N$ [4–7], this interpretation effectively addresses the mass inversion problem. Even more promising than the deuteron and $\Lambda(1405)$ is the discovery of the $X(3872)$ [8,9]. Because of its charge and its proximity to

the $\bar{D}D$ threshold in terms of mass, the molecular state interpretation of $\bar{D}D$ was proposed [10–12]. In 2019, the LHCb Collaboration reported three narrow hidden-charm pentaquark states, named $P_c(4312)$, $P_c(4440)$, and $P_c(4457)$ [13]. Their spectroscopic properties and decay widths find a compelling explanation within the context of $\Sigma_c\bar{D}^{(*)}$ molecular states [14–18]. More recently, the LHCb Collaboration unveiled another novel hidden-charm pentaquark state, $P_{cs}(4459)$ [19], which can be assigned as a $\Xi_c\bar{D}^*$ molecular state [20–25]. The existence of additional candidates for molecular states has been explored in Ref. [26].

Inspired by the above observation and their interpretation as molecules, it is interesting to study whether there exist hadronic molecular states corresponding to Ξ baryon. At present, there are 11 Ξ baryons listed in the review of the Particle Data Group (PDG) [1]. The ground-state octet and decuplet baryons, the $\Xi(1320)$ and the $\Xi(1530)$, are well established with four star ratings and can easily be fitted into the conventional quark model. For the states $\Xi(1690)$, $\Xi(1820)$, $\Xi(2030)$, and $\Xi(2120)$, there exist many different interpretations, such as qqq states and molecular systems [27–33]. In particular, we will show that there is good reason to believe that the state $\Xi(2030)$ is a P -wave bound state in this work.

The $\Xi(2030)$ is a three-star state and has a mass of 2023 ± 5 MeV and a width of 20_{-5}^{+15} MeV [1]. An early experimental analysis [34] suggested that the spin of the $\Xi(2030)$ should be $J \geq 5/2$. Before the experimental

^{*}Corresponding author: huangy2019@swjtu.edu.cn

Published by the American Physical Society under the terms of the [Creative Commons Attribution 4.0 International license](https://creativecommons.org/licenses/by/4.0/). Further distribution of this work must maintain attribution to the author(s) and the published article's title, journal citation, and DOI. Funded by SCOAP³.

observation of the $\Xi(2030)$, Samios *et al.* predicted that according to the $SU(3)$ flavor symmetry the $\Xi(2030)$ is most likely the partner of the $N(1680)$, $\Lambda(1820)$, and $\Sigma(1915)$ with $J^P = 5/2^+$ [35]. The constituent quark model calculations in Ref. [30] indicated that the $\Xi(2030)$ might be a candidate for the $J^P = 5/2^+$ state or the $J^P = 7/2^+$ state. However, the strong decay analysis based on the experimental measurements disfavors the assignment of the $\Xi(2030)$ as a member of the $5/2^+$ octet [36]. Also, the strong decay analysis in the chiral quark model [32] concludes that the $\Xi(2030)$ could not be assigned as any spin-parity $J^P = 7/2^+$ states or pure $J^P = 5/2^+$ state, It seems to favor the $J^P = 3/2^+$ assignment. However, this conflicts with the early analysis of the data [34].

Compared with the $\Xi(2030)$, the experimental information on the one-star state $\Xi(2120)$ is scarce [1]: both the spin parity and the width are not known experimentally. The $\Xi(2120)$ was first observed in the $\bar{K}\Lambda$ invariant mass spectrum by the Amsterdam-CERN-Nijmegen-Oxford Collaboration [37], and later confirmed by the French-Soviet and CERN-Soviet Collaboration [38] in the 1970s, where a mass of about 2120 MeV and a width of about 20 MeV was suggested by those observations with poor statistics. There exist a few theoretical studies about the nature of the $\Xi(2120)$. A study in the chiral unitary approach suggested that a pole around 2100 MeV can be produced from the interaction between pseudoscalar/vector mesons and baryons with $J^P = 1/2^-$ and $3/2^-$, which can be associated with the $\Xi(2120)$ [39,40]. In Ref. [33] the $I(J^P) = 1/2(3/2^-)$ state located at $2046 - i8.2$ MeV is identified as a meson-baryon molecule that can be associated with the $\Xi(2120)$. Meanwhile, it is claimed that the $\Xi(2120)$ have a big $\bar{K}\Sigma$ component.

Based on the preceding discussion, it is evident that the $\Xi(2030)$ cannot be easily explained as a qqq state. The mass of the $\Xi(2030)$ closely approaches the thresholds for $\bar{K}^*\Sigma$ and $\rho\Xi$, suggesting a possible interpretation as a bound state of $\bar{K}^*\Sigma/\rho\Xi$. Furthermore, we observe strong coupling between the $\bar{K}^*\Sigma$ and $\rho\Xi$ channels with other channels such as $\bar{K}^*\Lambda$, $\omega\Xi$, and $\phi\Xi$ [33]. And the $\Xi(2120)$ has previously been interpreted as a $\bar{K}^*\Sigma - \rho\Xi - \bar{K}^*\Lambda - \phi\Xi - \omega\Xi$ molecular state in the literature [33,39,40]. Therefore, it is plausible to interpret the $\Xi(2030)$ and $\Xi(2120)$ baryons as two distinct bound states originating from the $\bar{K}^*\Sigma - \rho\Xi - \bar{K}^*\Lambda - \phi\Xi - \omega\Xi$ interaction with differing quantum numbers. Assuming this interpretation, the $\Xi(2030)$ is, at the very least, a P -wave bound state. Extensive evidence, as presented in Refs. [41–44], supports the existence of several P -wave bound state candidates with molecular components such as $B_s^{(*)}\pi - \bar{B}^{(*)}K$, $\bar{D}^*\Sigma_c$, $D_s\bar{D}_{s0}(2370)$, and $\bar{B}^{(*)}N$.

In this study, we explore the interactions of $\bar{K}^*\Sigma - \rho\Xi - \bar{K}^*\Lambda - \phi\Xi - \omega\Xi$ and aim to elucidate the properties of the baryons $\Xi(2030)$ and $\Xi(2120)$. In addition, we predict the

existence of other molecular states composed of $\bar{K}^*\Sigma - \rho\Xi - \bar{K}^*\Lambda - \phi\Xi - \omega\Xi$ components. This paper is organized as follows. In Sec. II, we will present the theoretical formalism. In Sec. III, the numerical result will be given, followed by discussions and conclusions in Sec. III.

II. THEORETICAL FORMALISM

In this work, we search for possible vector meson-baryon molecular states in the one-boson exchange (OBE) model, which has been successfully employed to study the NN interaction [45]. With great success in reproducing the NN data, the OBE model was also extended to study the systems with heavy flavors in Refs. [46–51]. Especially, it is a powerful tool in reproducing the observed pentaquarks [46]. Our calculation is based on a nonrelativistic approach in the OBE model, which only contains the one-meson-exchange diagrams. Here, the channels involved are $\bar{K}^*\Sigma, \rho\Xi, \bar{K}^*\Lambda, \phi\Xi$, and $\omega\Xi$, and the relevant Feynman diagrams are illustrated in Fig. 1.

To compute the potential kernel, the gauge invariant hidden local symmetry Lagrangian for the coupling of vector mesons to the baryon octet given by [33,52–54]

$$\begin{aligned} \mathcal{L}_{VBB} = & -g\{\langle\bar{B}\gamma_\mu[V^\mu, B]\rangle + \langle\bar{B}\gamma_\mu B\rangle\langle V^\mu\rangle \\ & + \frac{1}{4M}(F\langle\bar{B}\sigma_{\mu\nu}[V^{\mu\nu}, B]\rangle + D\langle\bar{B}\sigma_{\mu\nu}\{V^{\mu\nu}, B\}\rangle)\}, \end{aligned} \quad (1)$$

where the M represent the masses of the baryon and $\langle\cdots\rangle$ refers to an $SU(3)$ trace. $\{A, B\} = AB + BA$ and $[A, B] = AB - BA$. The constants $D = 2.4$ and $F = 0.82$ were found to reproduce well the magnetic moments of the baryons [55]. The tensor field of the vector mesons $V^{\mu\nu} = \partial^\mu V^\nu - \partial^\nu V^\mu$ and $\sigma^{\mu\nu} = \frac{i}{2}(\gamma^\mu\gamma^\nu - \gamma^\nu\gamma^\mu)$. B and V^μ are the $SU(3)$ baryon octet and vector meson matrices, respectively,

$$B = \begin{pmatrix} \frac{1}{\sqrt{2}}\Sigma^0 + \frac{1}{\sqrt{6}}\Lambda & \Sigma^+ & p \\ \Sigma^- & -\frac{1}{\sqrt{2}}\Sigma^0 + \frac{1}{\sqrt{6}}\Lambda & n \\ \Xi^- & \Xi^0 & -\frac{2}{\sqrt{6}}\Lambda \end{pmatrix}, \quad (2)$$

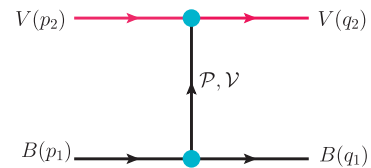


FIG. 1. The Feynman diagrams for the vector meson-baryon interaction via t -channel mesons exchange.

$$V_\mu = \begin{pmatrix} \frac{1}{\sqrt{2}}(\rho^0 + \omega) & \rho^+ & K^{*+} \\ \rho^- & \frac{1}{\sqrt{2}}(-\rho^0 + \omega) & K^{*0} \\ K^{*-} & \bar{K}^{*0} & \phi \end{pmatrix}_\mu \quad (3)$$

The Lagrangians involving the interaction of the three-vector mesons vertex VVV and the coupling of two vector mesons to pseudoscalar meson vertex VVP are given by [56–59]

$$\mathcal{L}_{VVV} = ig \langle (V^\mu \partial_\nu V_\mu - \partial_\nu V_\mu V^\mu) V^\nu \rangle, \quad (4)$$

$$\mathcal{L}_{VVP} = \frac{G'}{\sqrt{2}} \epsilon^{\mu\nu\alpha\beta} \langle \partial_\mu V_\nu \partial_\alpha V_\beta P \rangle, \quad (5)$$

where $\epsilon^{\mu\nu\alpha\beta}$ is the Levi-Civita tensor with $\epsilon^{0123} = 1$. The P is the standard $SU(3)$ pseudoscalar meson octet matrix [56–58]

$$P = \begin{pmatrix} \frac{1}{\sqrt{2}}\pi^0 + \frac{1}{\sqrt{6}}\eta_8 & \pi^+ & K^+ \\ \pi^- & -\frac{1}{\sqrt{2}}\pi^0 + \frac{1}{\sqrt{6}}\eta_8 & K^0 \\ K^- & \bar{K}^0 & -\frac{2}{\sqrt{6}}\eta_8 \end{pmatrix}, \quad (6)$$

where $\eta_8 = \frac{2\sqrt{2}}{3}\eta - \frac{1}{3}\eta'$ [56,57]. The coupling constant $G' = \frac{3g^2}{4\pi^2 f}$ with $g' = -\frac{G_V m_p}{\sqrt{2}f^2}$, $G_V = 55$ MeV, and $f = 93$ MeV. The coupling constant g can be fixed from the strong decay width of $K^* \rightarrow K\pi$. Note that the relationship between the coupling constants G_V and G' is established by computing $V \rightarrow V\gamma$ (where V signifies a vector meson) [60], and the accurate value of $G_V = 55$ GeV is derived from the computation of decay $\rho \rightarrow \pi\pi$ [61]. With the help of the following Lagrangian:

$$\mathcal{L}_{VPP} = -ig \langle [P, \partial_\mu P] V^\mu \rangle, \quad (7)$$

the two body decay width $\Gamma(K^{*+} \rightarrow K^0\pi^+)$ is related to g as

$$\Gamma(K^{*+} \rightarrow K^0\pi^+) = \frac{g^2}{6\pi m_{K^{*+}}^2} \mathcal{P}_{\pi K^*}^3 = \frac{2}{3} \Gamma_{K^{*+}}, \quad (8)$$

where the $\mathcal{P}_{\pi K^*}$ is the three momentum of the π in the rest frame of the K^* . Using the experimental strong decay width $\Gamma_{K^{*+}} = 50.3 \pm 0.8$ MeV and the masses of the particles [1], we obtain $g = 4.64$.

To compute the potential corresponding to Fig. 1(a), the chiral Lagrangian for meson-baryon interactions is needed [62–64]

$$\begin{aligned} \mathcal{L}_{PBB} = & -\frac{\sqrt{2}D_1 + F_1}{f} \frac{1}{2} \langle \bar{B} \gamma_\mu \gamma_5 \partial^\mu P B \rangle \\ & -\frac{\sqrt{2}D_1 - F_1}{f} \frac{1}{2} \langle \bar{B} \gamma_\mu \gamma_5 B \partial^\mu P \rangle, \end{aligned} \quad (9)$$

where $F_1 = 0.51$, $D_1 = 0.75$, and $f = 93$ MeV [64]. It is worth noting that the parameters can also take the values $F_1 = 0.46$, $D_1 = 0.8$, which were derived solely by fitting experimental data for the decay processes of n into p , Λ into p , Ξ into Λ , and Σ into n using the least squares method [65]. Note that they represent only one specific case when calculated with $F_1 = 0.51$, $D_1 = 0.75$ by combining theoretical calculations and experimental data [66].

Because hadrons are not pointlike particles, we need to include the form factors in evaluating the scattering amplitudes. For the t -channel mesons exchange, we would like to apply a widely used pole form factor, which is

$$\mathcal{F}_i = \frac{\Lambda^2 - m_i^2}{\Lambda^2 - q^2} = \frac{\Lambda^2 - m_i^2}{\tilde{\Lambda}^2 + q^2}, \quad (10)$$

where m_i and q are the masses and the four-momenta of exchanged mesons, respectively. The cutoff $\Lambda = m_i + \alpha \Lambda_{\text{QCD}}$ with $\Lambda_{\text{QCD}} = 220$ MeV, and $\tilde{\Lambda} = \Lambda^2 - (m_f^V - m_i^V)^2$. The parameter α is taken as a parameter and discussed later.

Putting all the pieces together, the effective potentials can easily be computed. For the t -channel mesons exchange, the potential are written as

$$\mathcal{V}_j^t = \sum_j \prod_{k=1,2} \mathcal{C}_{j_k} \left(\sum_{\mathcal{H}=V,P} \mathcal{M}_j^{\mathcal{H}} \right), \quad (11)$$

with

$$\begin{aligned} \mathcal{M}_j^V = & -ig \bar{u}_{\lambda_1'}(q_1) \left[\mathcal{X}_V g \gamma_\eta - \frac{\mathcal{Y}_V}{4M_\Sigma} (\gamma_\eta \not{q}_t - \not{q}_t \gamma_\eta) \right] \\ & \times u_{\lambda_1}(p_1) \frac{(-g'^\sigma + q_t^\sigma / m_V^2)}{q_t^2 - m_V^2} [(q_t - p_2) \cdot \epsilon^\dagger \\ & \times \epsilon_\sigma - (q_t + q_2) \cdot \epsilon \epsilon_\sigma^\dagger + (p_2 + q_2)_\sigma \epsilon^\dagger \cdot \epsilon], \end{aligned} \quad (12)$$

$$\begin{aligned} \mathcal{M}_j^P = & \frac{G'}{f} \bar{u}_{\lambda_1'}(q_1) \not{q}_t \gamma_5 u_{\lambda_1}(p_1) \frac{1}{q_t^2 - m_P^2} \epsilon_{\mu\nu\alpha\beta} \\ & \times (\mathcal{Z}_P q_2^\mu \epsilon_\nu^\dagger p_2^\alpha \epsilon_\beta + \mathcal{S}_P p_2^\mu \epsilon_\nu^\dagger q_2^\alpha \epsilon_\beta^\dagger), \end{aligned} \quad (13)$$

where u is the Dirac spinor of baryon and ϵ_σ is the polarization vector of the meson. $q_t = q_2 - p_2$ is the four-momenta of the t -channel exchange mesons, and $\not{q}_t = q_t^\mu \gamma_\mu$. The index j stands by the different channels, and j_1 and j_2 are its initial state and final state, respectively. The coefficients \mathcal{X}_V , \mathcal{Y}_V for vector mesons exchange potential and \mathcal{Z}_P , \mathcal{S}_P for pseudoscalar meson exchange potentials are computed in Table I. \mathcal{C}_{j_k} is the isospin coefficient, which is calculated from the following isospin assignments [4]:

TABLE I. The coefficients for the t -channel mesons exchange potential.

Channel (j)	\mathcal{I}_V			\mathcal{J}_V			\mathcal{Z}_P			\mathcal{S}_P			Channel (j)	\mathcal{I}_V	\mathcal{J}_V	\mathcal{Z}_P	\mathcal{S}_P
	ρ	ω	ϕ	ρ	ω	ϕ	η	η'	π	η	η'	π		\bar{K}^*	\bar{K}^*	\bar{K}	
$K^{*-}\Sigma^+ \rightarrow K^{*-}\Sigma^+$	1	1	-1	F	D	0	$\frac{4D_1}{27}$	$\frac{D_1}{54}$	$\frac{F_1}{2}$	$-\frac{8D_1}{27}$	$-\frac{D_1}{27}$	0	$K^{*-}\Sigma^+ \rightarrow \rho^+\Xi^-$	0	0	0	0
$\bar{K}^{*0}\Sigma^0 \rightarrow \bar{K}^{*0}\Sigma^0$	0	1	-1	0	D	0	$\frac{4D_1}{27}$	$\frac{D_1}{54}$	0	$-\frac{8D_1}{27}$	$-\frac{D_1}{27}$	0	$K^{*-}\Sigma^+ \rightarrow \rho^0\Xi^0$	$-\frac{1}{\sqrt{2}}$	$-\frac{F+D}{\sqrt{2}}$	0	$\frac{D_1}{2\sqrt{2}}$
$K^{*-}\Sigma^+ \rightarrow \bar{K}^{*0}\Sigma^0$	$-\sqrt{2}$	0	0	$-\sqrt{2}F$	0	0	0	0	$-\frac{F_1}{\sqrt{2}}$	0	0	0	$\bar{K}^{*0}\Sigma^0 \rightarrow \rho^0\Xi^0$	$-\frac{1}{2}$	$-\frac{F+D}{2}$	0	$\frac{F_1}{4}$
$\bar{K}^{*0}\Lambda \rightarrow \bar{K}^{*0}\Lambda$	0	$\sqrt{2}$	-1	0	$\frac{\sqrt{2}D}{3}$	$-\frac{4D}{3}$	$-\frac{4D_1}{27}$	$-\frac{D_1}{54}$	0	$\frac{8D_1}{27}$	$\frac{D_1}{27}$	0	$\bar{K}^{*0}\Sigma^0 \rightarrow \rho^+\Xi^-$	$-\frac{1}{2}$	$-\frac{F+D}{2}$	0	$\frac{D_1}{2\sqrt{2}}$
$\rho^+\Xi^- \rightarrow \rho^+\Xi^-$	-1	0	0	$D-F$	0	0	$-\frac{2D_1}{27}$	$-\frac{D_1}{108}$	$-\frac{F_1}{4}$	$-\frac{2D_1}{27}$	$-\frac{D_1}{108}$	$\frac{F_1}{4}$	$\bar{K}^{*0}\Lambda \rightarrow \rho^+\Xi^-$	$-\frac{\sqrt{6}}{2}$	$\frac{D-3F}{\sqrt{6}}$	0	$\frac{\sqrt{6}F_1}{4}$
$\rho^0\Xi^0 \rightarrow \rho^0\Xi^0$	0	0	0	0	0	0	$-\frac{2D_1}{27}$	$-\frac{D_1}{108}$	0	$-\frac{2D_1}{27}$	$-\frac{D_1}{108}$	0	$\bar{K}^{*0}\Lambda \rightarrow \rho^+\Xi^-$	$-\frac{\sqrt{6}}{2}$	$\frac{D-3F}{\sqrt{6}}$	0	$\frac{\sqrt{6}F_1}{4}$
$\rho^+\Xi^- \rightarrow \rho^0\Xi^0$	$-\sqrt{2}$	0	0	$\sqrt{2}(D-F)$	0	0	0	0	$\frac{D_1}{2\sqrt{2}}$	0	0	$-\frac{D_1}{2\sqrt{2}}$	$K^{*-}\Sigma^+ \rightarrow \omega\Xi^0$	$-\frac{1}{\sqrt{2}}$	$-\frac{D+F}{\sqrt{2}}$	0	$\frac{F_1}{2\sqrt{2}}$
$\omega\Xi^0 \rightarrow \omega\Xi^0$	0	0	0	0	0	0	$-\frac{2D_1}{9}$	$-\frac{D_1}{36}$	0	0	0	0	$\bar{K}^{*0}\Sigma^0 \rightarrow \omega\Xi^0$	$\frac{1}{2}$	$\frac{D+F}{2}$	0	$-\frac{D_1}{4}$
$\phi\Xi^0 \rightarrow \phi\Xi^0$	0	0	0	0	0	0	$\frac{4D_1}{9}$	$\frac{D_1}{18}$	0	0	0	0	$\bar{K}^{*0}\Lambda \rightarrow \omega\Xi^0$	$-\frac{\sqrt{3}}{2}$	$\frac{D-3F}{2\sqrt{3}}$	0	$-\frac{D_1}{4\sqrt{3}}$
$K^{*-}\Sigma^+ \rightarrow \bar{K}^{*0}\Lambda$	0	0	0	$\frac{\sqrt{6}D}{3}$	0	0	0	0	$\frac{D_1}{\sqrt{6}}$	0	0	0	$K^{*-}\Sigma^+ \rightarrow \phi\Xi^0$	1	1	$\frac{F_1}{2}$	0
$\bar{K}^{*0}\Sigma^0 \rightarrow \bar{K}^{*0}\Lambda$	0	0	0	$-\frac{D}{\sqrt{3}}$	0	0	0	0	$-\frac{D_1}{2\sqrt{3}}$	0	0	0	$\bar{K}^{*0}\Sigma^0 \rightarrow \phi\Xi^0$	$-\frac{1}{\sqrt{2}}$	$-\frac{D+F}{\sqrt{2}}$	$-\frac{F_1}{2\sqrt{2}}$	0
$\rho^+\Xi^- \rightarrow \omega\Xi^0$	0	0	0	0	0	0	0	0	$-\frac{F_1}{2\sqrt{2}}$	0	0	$-\frac{F_1}{2\sqrt{2}}$	$\bar{K}^{*0}\Lambda \rightarrow \phi\Xi^0$	$\frac{\sqrt{6}}{2}$	$\frac{3F-D}{\sqrt{6}}$	$-\frac{D_1}{2\sqrt{6}}$	0
$\rho^0\Xi^0 \rightarrow \omega\Xi^0$	0	0	0	0	0	0	0	0	$-\frac{D_1}{4}$	0	0	$-\frac{D_1}{4}$					
$\rho^+\Xi^- \rightarrow \phi\Xi^0$	0	0	0	0	0	0	0	0	0	0	0	0					
$\rho^0\Xi^0 \rightarrow \phi\Xi^0$	0	0	0	0	0	0	0	0	0	0	0	0					
$\omega\Xi^0 \rightarrow \phi\Xi^0$	0	0	0	0	0	0	0	0	0	0	0	0					

$$\begin{aligned} \begin{pmatrix} p \\ n \end{pmatrix} &= \begin{pmatrix} |\frac{1}{2}, \frac{1}{2}\rangle \\ |\frac{1}{2}, -\frac{1}{2}\rangle \end{pmatrix}, \quad \begin{pmatrix} K^{*-} \\ \bar{K}^{*0} \end{pmatrix} = \begin{pmatrix} |-\frac{1}{2}, -\frac{1}{2}\rangle \\ |\frac{1}{2}, \frac{1}{2}\rangle \end{pmatrix}, \\ \begin{pmatrix} \rho^+ \\ \rho^0 \\ \rho^- \end{pmatrix} &= \begin{pmatrix} |1, 1\rangle \\ |1, 0\rangle \\ |1, -1\rangle \end{pmatrix}, \quad \begin{pmatrix} \Sigma^+ \\ \Sigma^0 \\ \Sigma^- \end{pmatrix} = \begin{pmatrix} |-1, 1\rangle \\ |1, 0\rangle \\ |1, -1\rangle \end{pmatrix}, \\ \begin{pmatrix} \Xi^0 \\ \Xi^- \end{pmatrix} &= \begin{pmatrix} |\frac{1}{2}, \frac{1}{2}\rangle \\ |-\frac{1}{2}, -\frac{1}{2}\rangle \end{pmatrix}, \end{aligned}$$

and we collect them in Table II.

In the above equation, the polarization vector $e^\mu(s)$ represent the wave function of the spin-one field and can be expressed as

$$e^\mu(s=0) = \begin{pmatrix} 0 \\ 0 \\ 0 \\ 1 \end{pmatrix}; \quad e^\mu(s=\pm) = \frac{1}{\sqrt{2}} \begin{pmatrix} 0 \\ \mp 1 \\ -i \\ 0 \end{pmatrix}. \quad (14)$$

TABLE II. C_{jk} is the isospin coefficient with $k=1, 2$.

j_k	$\Sigma\bar{K}^*$		$\Lambda\bar{K}^*$	$\Xi\rho$		$\Xi\omega$	$\Xi\phi$
	Σ^+K^{*-}	$\Sigma^0\bar{K}^{*0}$	$\Lambda\bar{K}^{*0}$	$\Xi^-\rho^+$	$\Xi^0\rho^0$	$\Xi^0\omega$	$\Xi^0\phi$
C_{jk}	$\sqrt{\frac{2}{3}}$	$-\frac{1}{\sqrt{3}}$	1	$-\sqrt{\frac{2}{3}}$	$\frac{1}{\sqrt{3}}$	1	1

The $u_{s_1}(p_1)$ and $\bar{u}_{s'_1}(q_1)$ stand for the spin wave function of baryons. In this work we adopt the Dirac spinor as

$$u(\vec{q}, s) = \sqrt{\frac{E+m}{2m}} \begin{pmatrix} 1 \\ \frac{\vec{\sigma}\cdot\vec{q}}{E+m} \end{pmatrix} \chi_s, \quad (15)$$

$$\bar{u}(\vec{q}, s) = u^\dagger(\vec{q}, s)\gamma^0 = \chi_s^\dagger \sqrt{\frac{E+m}{2m}} \left(1 - \frac{\vec{\sigma}\cdot\vec{q}}{E+m} \right), \quad (16)$$

where $\chi_{1/2} = (1, 0)^\dagger$ and $\chi_{-1/2} = (0, 1)^\dagger$, and index $\pm 1/2$ is the third component of the spin s . E , \vec{q} , and m are the energy, three-momenta, and masses of baryons, respectively, and they have on-shell relation $E^2 = \vec{q}^2 + m^2$.

By considering the nonrealistic approximation and keeping the terms up to the order of $1/m^2$, the scattering amplitudes are

$$\begin{aligned} \mathcal{M}_j^P &= \frac{G'}{f} \frac{\vec{\sigma}\cdot\vec{q}}{\vec{q}^2 + \omega_p^2} (\mathcal{Z}_P + \mathcal{S}_P) \left[(m_f^V - m_i^V) \vec{k} \cdot (\vec{\epsilon} \times \vec{\epsilon}^\dagger) \right. \\ &\quad \left. - \frac{(m_f^V + m_i^V)}{2} \vec{q} \cdot (\vec{\epsilon} \times \vec{\epsilon}^\dagger) \right], \end{aligned} \quad (17)$$

$$\mathcal{M}_j^V = \frac{ig}{\vec{q}^2 + \omega_V^2} \left(-g\mathcal{X}_V\mathcal{T}_1 + \frac{\mathcal{Y}_V}{4m_i^B} \mathcal{T}_2 \right), \quad (18)$$

with

$$\omega_P^2 = m_P^2 - (m_f^V - m_i^V)^2, \quad (19)$$

$$\omega_V^2 = m_V^2 - (m_f^V - m_i^V)^2, \quad (20)$$

$$\begin{aligned} \mathcal{T}_1 = & \frac{m_f^V - m_i^V}{m_V^2} \vec{A} \cdot \vec{q} + \left(\frac{(m_i^B + m_f^B)}{2m_i^B m_f^B} \vec{\sigma}_2 \cdot \vec{k} + \frac{(m_i^B - m_f^B)}{4m_i^B m_f^B} \right. \\ & \left. \times \vec{\sigma}_2 \cdot \vec{q} \right) \left[\vec{\sigma}_1 \cdot \vec{A} - \frac{(m_f^{V2} - m_i^{V2})}{m_V^2} (\vec{\sigma}_1 \cdot \vec{q}) \epsilon^\dagger \cdot \epsilon \right] \\ & + \left(1 + \frac{\vec{k}^2 - \frac{1}{4}\vec{q}^2}{4m_f^B m_i^B} \right) \left[1 - \frac{(m_f^V - m_i^V)^2}{m_V^2} \right] \\ & \times (m_f^V + m_i^V) \epsilon^\dagger \cdot \epsilon, \end{aligned} \quad (21)$$

$$\begin{aligned} \mathcal{T}_2 = & [(m_f^V - m_i^V)(\vec{\sigma}_1 \cdot \vec{A}) - (m_f^V + m_i^V) \epsilon^\dagger \cdot \epsilon (\vec{\sigma}_1 \cdot \vec{q})] \\ & \times \left(\frac{(m_i^B - m_f^B)}{m_i^B m_f^B} \vec{\sigma}_2 \cdot \vec{k} + \frac{(m_i^B + m_f^B)}{2m_i^B m_f^B} \vec{\sigma}_2 \cdot \vec{q} \right), \end{aligned} \quad (22)$$

where $\vec{A} = (\frac{3}{2}\vec{q} - \vec{k}) \cdot \vec{\epsilon}^\dagger \vec{\epsilon} - (\frac{3}{2}\vec{q} + \vec{k}) \cdot \vec{\epsilon} \vec{\epsilon}^\dagger + 2\vec{k} \epsilon^\dagger \cdot \epsilon$, and m_i and m_f are the masses of the initial states and final

states, respectively. Variables in the above functions denote $\vec{q} = \vec{q}_2 - \vec{p}_2$ and $\vec{k} = \frac{1}{2}(\vec{q}_2 + \vec{p}_2)$. Note that the ω_P and ω_V are always positive for considering systems.

Now we make the following Fourier transformation to get the effective potential $V(r)$ in the coordinate space:

$$\mathcal{V}_j(r) = \int \frac{d^3\vec{q}}{(2\pi)^3} e^{-i\vec{q}\cdot\vec{r}} \mathcal{V}_j(\vec{q}) \mathcal{F}^2(\vec{q}), \quad (23)$$

where the momentum-space potentials $\mathcal{V}(\vec{q})$ is obtained by utilizing the Breit approximation [67,68]

$$\mathcal{V}_j(\vec{q}) = -\frac{\mathcal{M}_j^t}{\sqrt{\prod_i 2m_i \prod_f 2m_f}}. \quad (24)$$

Thus, the expressions of corresponding coordinate-space potentials can be obtained with the relations

$$\begin{aligned} \mathcal{F} \left\{ \frac{1}{\vec{q}^2 + a^2} \left(\frac{\Lambda^2 - m^2}{b^2 + \vec{q}^2} \right)^2 \right\} &= Y_1(\Lambda, m, a, b, r), \\ \mathcal{F} \left\{ \frac{\vec{q}^2}{\vec{q}^2 + a^2} \left(\frac{\Lambda^2 - m^2}{b^2 + \vec{q}^2} \right)^2 \right\} &= -\nabla_r^2 Y_1(\Lambda, m, a, b, r), \\ \mathcal{F} \left\{ \frac{\vec{k}^2}{\vec{q}^2 + a^2} \left(\frac{\Lambda^2 - m^2}{b^2 + \vec{q}^2} \right)^2 \right\} &= \frac{1}{4} \nabla_r^2 Y_1(\Lambda, m, a, b, r) - \frac{\mathcal{F}_1}{2}, \\ \mathcal{F} \left\{ \frac{i\vec{\sigma} \cdot (\vec{q} \times \vec{k})}{\vec{q}^2 + a^2} \left(\frac{\Lambda^2 - m^2}{b^2 + \vec{q}^2} \right)^2 \right\} &= \vec{\sigma} \cdot \vec{L} \left(\frac{1}{r} \frac{\partial}{\partial r} \right) Y_1(\Lambda, m, a, b, r), \\ \mathcal{F} \left\{ \frac{(\vec{A} \cdot \vec{q})(\vec{B} \cdot \vec{q})}{\vec{q}^2 + a^2} \left(\frac{\Lambda^2 - m^2}{b^2 + \vec{q}^2} \right)^2 \right\} &= \frac{1}{3} (\vec{A} \cdot \vec{B}) (-\nabla_r^2 Y_1(\Lambda, m, a, b, r)) + \frac{1}{3} S(\hat{r}, \vec{A}, \vec{B}) \left(-r \frac{\partial}{\partial r} \frac{1}{r} \frac{\partial}{\partial r} Y_1(\Lambda, m, a, b, r) \right), \\ \mathcal{F} \left\{ \frac{(\vec{A} \cdot \vec{k})(\vec{B} \cdot \vec{q})}{\vec{q}^2 + a^2} \left(\frac{\Lambda^2 - m^2}{b^2 + \vec{q}^2} \right)^2 \right\} &= \frac{1}{3} (\vec{A} \cdot \vec{B}) (\nabla_r^2 Y_1(\Lambda, m, a, b, r)) - \frac{1}{3} \left(-r \frac{\partial}{\partial r} \frac{1}{r} \frac{\partial}{\partial r} Y_1(\Lambda, m, a, b, r) \right) \\ &\quad - \frac{2}{3} \left(\frac{\partial}{\partial r} Y_1(\Lambda, m, a, b, r) \right) (S(\hat{r}, \vec{A}, \vec{B}) + \vec{A} \cdot \vec{B}) \frac{\partial}{\partial r}, \\ \mathcal{F} \left\{ \frac{\vec{k} \cdot \vec{q}}{\vec{q}^2 + a^2} \left(\frac{\Lambda^2 - m^2}{b^2 + \vec{q}^2} \right)^2 \right\} &= ir \nabla Y_1(\Lambda, m, a, b, r), \\ \mathcal{F} \left\{ \frac{(\vec{A} \cdot \vec{k})(\vec{B} \cdot \vec{k})}{\vec{q}^2 + a^2} \left(\frac{\Lambda^2 - m^2}{b^2 + \vec{q}^2} \right)^2 \right\} &= -\frac{1}{4} (\vec{A} \cdot \vec{B}) \nabla^2 Y_1(\Lambda, m, a, b, r) + \frac{1}{3} (S(\hat{r}, \vec{A}, \vec{B}) + \vec{A} \cdot \vec{B}) \left[\left(\frac{2}{r} - \frac{\partial}{\partial r} \right) Y_1 \frac{\partial}{\partial r} - Y_1 \nabla^2 \right], \end{aligned} \quad (25)$$

where \mathcal{F} denotes the Fourier transformation, $\nabla_r^2 = \frac{1}{r^2} \frac{\partial}{\partial r} r^2 \frac{\partial}{\partial r}$, $\vec{\sigma} \cdot \vec{L}$ is the spin-orbital operator, and $S(\hat{r}, \vec{x}, \vec{y}) = 3(\hat{r} \cdot \vec{x})(\hat{r} \cdot \vec{y}) - \vec{x} \cdot \vec{y}$ is the tensor operator. The function

$$Y_1(\Lambda, m, a, b, r) = \left(\frac{\Lambda^2 - m^2}{b^2 - a^2} \right)^2 \left[\frac{1}{4\pi r} (e^{-ar} - e^{-br}) - \frac{b^2 - a^2}{8\pi b} e^{-br} \right] \quad (26)$$

and

$$\mathcal{F}_1 = \{ \nabla_r^2, Y_1(\Lambda, m, a, r) \} = \nabla_r^2 Y_1(\Lambda, m, a, r) + Y_1(\Lambda, m, a, r) \nabla_r^2. \quad (27)$$

TABLE III. The matrix elements of two-body interaction operators for VB systems.

$VB \rightarrow VB$	$1/2^-$	$3/2^-$	$5/2^-$	$1/2^+$	$3/2^+$	$5/2^+$
\mathcal{Z}	$({}^2S_{1/2}, {}^4D_{1/2})$	$({}^4S_{3/2}, {}^2D_{3/2}, {}^4D_{3/2})$	$({}^2D_{5/2}, {}^4D_{5/2})$	$({}^2P_{1/2}, {}^4P_{1/2})$	$({}^2P_{3/2}, {}^4P_{3/2}, {}^4F_{3/2})$	$({}^4P_{5/2}, {}^2F_{5/2}, {}^4F_{5/2})$
$\vec{\sigma} \cdot (-i\vec{e}_{s_3} \times \vec{e}_{s_1})$	$\begin{pmatrix} -2 & 0 \\ 0 & 1 \end{pmatrix}$	$\begin{pmatrix} 1 & 0 & 0 \\ 0 & -2 & 0 \\ 0 & 0 & 1 \end{pmatrix}$	$\begin{pmatrix} -2 & 0 \\ 0 & 1 \end{pmatrix}$	$\begin{pmatrix} -2 & 0 \\ 0 & 1 \end{pmatrix}$	$\begin{pmatrix} -2 & 0 & 0 \\ 0 & 1 & 0 \\ 0 & 0 & 1 \end{pmatrix}$	$\begin{pmatrix} 1 & 0 & 0 \\ 0 & -2 & 0 \\ 0 & 0 & 1 \end{pmatrix}$
$S(\hat{r}, \vec{\sigma}, -i\vec{e}_{s_3} \times \vec{e}_{s_1})$	$\begin{pmatrix} 0 & -\sqrt{2} \\ -\sqrt{2} & -2 \end{pmatrix}$	$\begin{pmatrix} 0 & 1 & 2 \\ 1 & 0 & -1 \\ 2 & -1 & 0 \end{pmatrix}$	$\begin{pmatrix} 0 & \sqrt{\frac{2}{7}} \\ \sqrt{\frac{2}{7}} & \frac{10}{7} \end{pmatrix}$	$\begin{pmatrix} 0 & -\sqrt{2} \\ -\sqrt{2} & 2 \end{pmatrix}$	$\begin{pmatrix} 0 & \frac{1}{\sqrt{5}} & -\frac{3}{\sqrt{5}} \\ \frac{1}{\sqrt{5}} & \frac{8}{5} & \frac{6}{5} \\ -\frac{3}{\sqrt{5}} & \frac{6}{5} & -\frac{8}{5} \end{pmatrix}$	$\begin{pmatrix} -\frac{2}{5} & \sqrt{\frac{6}{5}} & \frac{4\sqrt{6}}{5} \\ \sqrt{\frac{6}{5}} & 0 & -\frac{2}{\sqrt{5}} \\ \frac{4\sqrt{6}}{5} & -\frac{2}{\sqrt{5}} & \frac{2}{5} \end{pmatrix}$
$\vec{e}_{s_1} \cdot \vec{e}_{s_3}$	$\begin{pmatrix} 1 & 0 \\ 0 & 1 \end{pmatrix}$	$\begin{pmatrix} 1 & 0 & 0 \\ 0 & 1 & 0 \\ 0 & 0 & 1 \end{pmatrix}$	$\begin{pmatrix} 1 & 0 \\ 0 & 1 \end{pmatrix}$	$\begin{pmatrix} 1 & 0 \\ 0 & 1 \end{pmatrix}$	$\begin{pmatrix} 1 & 0 & 0 \\ 0 & 1 & 0 \\ 0 & 0 & 1 \end{pmatrix}$	$\begin{pmatrix} 1 & 0 & 1 \\ 0 & 1 & 0 \\ 0 & 0 & 1 \end{pmatrix}$
$S(\hat{r}, \vec{e}_{s_1}, \vec{e}_{s_3})$	$\begin{pmatrix} 0 & -\sqrt{2} \\ -\sqrt{2} & 1 \end{pmatrix}$	$\begin{pmatrix} 0 & 1 & -1 \\ 1 & 0 & -1 \\ -1 & -1 & 0 \end{pmatrix}$	$\begin{pmatrix} 0 & \sqrt{\frac{2}{7}} \\ \sqrt{\frac{2}{7}} & -\frac{5}{7} \end{pmatrix}$	$\begin{pmatrix} 0 & -\sqrt{2} \\ -\sqrt{2} & 1 \end{pmatrix}$	$\begin{pmatrix} 0 & \frac{1}{\sqrt{5}} & -\frac{3}{\sqrt{5}} \\ \frac{1}{\sqrt{5}} & -\frac{4}{5} & -\frac{3}{5} \\ -\frac{3}{\sqrt{5}} & -\frac{3}{5} & \frac{4}{5} \end{pmatrix}$	$\begin{pmatrix} \frac{1}{5} & \sqrt{\frac{6}{5}} & -\frac{2\sqrt{6}}{5} \\ \sqrt{\frac{6}{5}} & 0 & -\frac{2}{\sqrt{5}} \\ -\frac{2\sqrt{6}}{5} & -\frac{2}{\sqrt{5}} & -\frac{1}{5} \end{pmatrix}$
$\vec{\sigma} \cdot \vec{L} \vec{e}_{s_1} \cdot \vec{e}_{s_3}$	$\begin{pmatrix} 0 & 0 \\ 0 & -3 \end{pmatrix}$	$\begin{pmatrix} 0 & 0 & 0 \\ 0 & 1 & -2 \\ 0 & -2 & -2 \end{pmatrix}$	$\begin{pmatrix} -\frac{2}{3} & -\frac{2\sqrt{14}}{3} \\ -\frac{2\sqrt{14}}{3} & -\frac{1}{3} \end{pmatrix}$	$\begin{pmatrix} \frac{2}{3} & -\frac{2\sqrt{2}}{3} \\ -\frac{2\sqrt{2}}{3} & -\frac{5}{3} \end{pmatrix}$	$\begin{pmatrix} -\frac{1}{3} & -\frac{2\sqrt{5}}{3} & 0 \\ -\frac{2\sqrt{5}}{3} & -\frac{2}{3} & 0 \\ 0 & 0 & -4 \end{pmatrix}$	$\begin{pmatrix} 1 & 0 & 0 \\ 0 & \frac{4}{3} & -\frac{4\sqrt{5}}{3} \\ 0 & -\frac{4\sqrt{5}}{3} & -\frac{7}{3} \end{pmatrix}$

To obtain numerical results, it is necessary to determine the values of spin-spin interactions and tensor force operators. To perform the calculations, we must provide the spin-orbital wave functions for the systems under discussion. In principle, the spin-orbital wave function can be uniquely defined by the orbital angular momentum (L), spin angular momentum (S), and total angular momentum (J). This wave function can be expressed as

$$|VB({}^{2S+1}L_J)\rangle = \sum_{m_S, m_L} C_{1/2m, 1m'}^{S, m_S} C_{S m_S, L m_L}^{J, M} \chi_{1/2m}^{\mu} |Y_{L, m_L}\rangle. \quad (28)$$

Here, $C_{ab, cd}^{e, f}$ represents the Clebsch-Gordan coefficient, and $|Y_{L, m_L}\rangle$ stands for the spherical harmonics function. M , m_S , and m_L are the third components of the total angular momentum (J), spin angular momentum (S), and orbital angular momentum (L), respectively. With this spin-orbital wave function, we can compute the spin-spin interaction operator and the tensor operator, and the results are compiled in Table III.

III. RESULTS AND DISCUSSIONS

In this study, we study the possibility of forming a molecular structure through $VB = (\bar{K}^* \Sigma / \rho \Xi / \bar{K}^* \Lambda / \phi \Xi / \omega \Xi)$ interactions. We employ the one-boson exchange model, which can be adapted to construct $VB \rightarrow VB$ interaction potentials. The corresponding scattering Feynman diagrams for the $VB \rightarrow VB$ reaction can be observed in Fig. 1, where we consider exchanges involving vector and pseudoscalar mesons in the t -channel. Utilizing the obtained effective

potential, we investigate the possible bound state by solving the nonrelativistic Schrödinger equation with the help of the Gaussian expansion method (GEM)

$$-\frac{1}{2\mu} \left[\nabla_r^2 - \frac{L(L+1)}{r^2} \right] \psi(\vec{r}) + V(r)\psi(\vec{r}) = E\psi(\vec{r}), \quad (29)$$

where μ represents the reduced mass of the discussed systems, calculated as $\mu = m_V m_B / (m_V + m_B)$. The specific case of $L = 0$ corresponds to the S -wave, a well-studied aspect in previous works. For a detailed procedure on solving the Schrödinger equation under the GEM framework, readers can refer to Ref. [69], which we omit discussing here.

Since vector mesons $V = (\bar{K}^* / \rho / \phi / \omega)$ and baryons $B = (\Sigma / \Lambda / \Xi)$ carry spin-parities 1^- and $1/2^+$, respectively, an S -wave bound state should have spin-parity $1/2^-$ or $3/2^-$. At present, the spin parity of $\Xi(2030)$ has not been fully determined [1]. Only an early experimental analysis suggested that the $\Xi(2030)$ should carry a spin $J \geq 5/2$ [34]. It requires that the $\Xi(2030)$ is at least a P -wave state if it is a VB molecular state. We would like to note that in our formalism, the partial wave decomposition is done only on J^P , and for a spin-parity state, it may contain contributions from different waves (see Table III). Here we do not distinguish the explicit contributions from which wave they come. Generally, the contributions with smaller L is more important for a certain spin parity close to threshold. In this work, we will consider the spin parities where at least the P -wave is involved. Since a system with $J \geq 7/2$ will be a D - (G -) wave state, only the isospin $1/2$ systems with $J \leq 5/2$ will be considered in this work. Given such constraints, possible bound states produced from the VB

TABLE IV. Possible bound states for the VB system with $\Lambda_i = m_i + \alpha 220$ MeV and different spin-parity assignments (in units of MeV). E is the eigenvalue. Notation \times means no binding solutions.

State	α	E	State	α	E
$J^P = 1/2^-$	1.7	-4.22	$J^P = 1/2^+$	1.0	-1.56
	1.8	-21.98		1.1	-23.83
	1.9	-62.96		1.2	-63.16
	2.0	-185.96		1.3	-83.90
$J^P = 3/2^+$	2.7	-0.13	$J^P = 3/2^-$	0.9	-4.20
	2.8	-28.20		1.0	-12.24
	2.9	-37.06		1.1	-16.95
	3.0	-48.31		1.2	-35.12
$J^P = 5/2^+$	3.4	-1.41	$J^P = 5/2^-$	\times	\times
	3.5	-9.68		\times	\times
	3.6	-10.15		\times	\times
	3.7	-41.48		\times	\times

interaction are listed in Table IV with the variation of the cutoff α .

From Table IV, we can find that a bound state in the $I(J^P) = 1/2(1/2^-)$ case is obtained. Its binding energy is 4.22 MeV when the cutoff α is taken as $\alpha = 1.7$. And the binding energies of the bound states produced from the VB interaction increase with the cutoff α . In other words, as the parameter α increases from small to large, the bound state becomes more and more tightly bound. Additionally, we find the presence of another S -wave bound state with $I(J^P) = 1/2(3/2^-)$. This state is relatively loosely bound compared to the bound state obtained in the $I(J^P) = 1/2(1/2^-)$ channel. This is mainly because the bound state appears in the $I(J^P) = 1/2(3/2^-)$ channel with a smaller α than that of the bound state in the $I(J^P) = 1/2(1/2^-)$ channel, and a smaller α corresponds to a loosely bound state. Obviously, these differences originate from the spin-orbit force contribution (see the fifth and seventh rows of Table III).

The existence of a bound state with a smaller value of α indicates that meson exchange contributions are most significant in the $J^P = 3/2^-$ channel, making it easily detectable. This suggests that for the $J^P = 3/2^-$ channel, the potential is considerably more attractive than that of the $J^P = 1/2^-$ case, aligning with the conclusions drawn from Hund's rule.

It is worth noting that the existence of possible S -wave VB bound states are also discussed in Refs. [33,39,40]. Especially in Ref. [33], a coupled-channel unitary approach was adopted, leading to the discovery of a dynamically generated meson-baryon molecular state with $I(J^P) = 1/2(3/2^-)$. This bound state is strongly suggested to be the experimental observed state $\Xi(2120)$ [33]. However, experimental information on the $\Xi(2120)$ is limited, making its assignment to a particular state challenging. In our

TABLE V. Different bound state components change with the cutoff parameter α .

J^P	α	$K^*\Sigma(\%)$	$K^*\Lambda(\%)$	$\Xi\rho(\%)$	$\Xi\omega(\%)$	$\Xi\phi(\%)$
$1/2^-$	1.7	99.1	0.1449	0.1524	4.064×10^{-5}	0.5310
	1.8	98.84	0.1929	0.1964	5.456×10^{-5}	0.6841
	1.9	98.52	0.2535	0.2499	7.229×10^{-5}	0.8708
	2.0	98.12	0.3290	0.3147	9.466×10^{-5}	1.0960
$3/2^-$	2.1	97.65	0.4223	0.3922	12.260×10^{-5}	1.3660
	0.9	99.89	5.11×10^{-7}	0.0023	3.96×10^{-7}	0.0094
	1.0	99.86	7.30×10^{-7}	0.0037	6.79×10^{-7}	0.0146
	1.1	99.82	9.92×10^{-7}	0.0058	11.13×10^{-7}	0.0217
$1/2^+$	1.2	99.77	12.92×10^{-7}	0.0088	17.63×10^{-7}	0.0313
	1.3	99.72	16.19×10^{-7}	0.0128	27.10×10^{-7}	0.0440
	1.0	99.98	0.003	0.0044	4.7×10^{-6}	0.0136
	1.1	99.97	0.005	0.0066	7.4×10^{-6}	0.0204
$3/2^+$	1.2	99.95	0.007	0.0096	11.2×10^{-6}	0.0295
	1.3	99.93	0.011	0.0134	16.6×10^{-6}	0.0415
	1.4	99.91	0.016	0.0185	23.9×10^{-6}	0.0570
	2.7	99.54	3.7×10^{-5}	0.459	4.1×10^{-5}	0.928
$5/2^+$	2.8	99.44	4.2×10^{-5}	0.557	5.3×10^{-5}	1.101
	2.9	99.33	4.8×10^{-5}	0.672	6.8×10^{-5}	1.299
	3.0	99.19	5.4×10^{-5}	0.807	8.6×10^{-5}	1.527
	3.1	99.03	6.1×10^{-5}	0.965	10.8×10^{-5}	1.787
$5/2^+$	3.4	99.67	2.1×10^{-5}	0.3277	3.5×10^{-4}	0.3411
	3.5	99.63	3.1×10^{-5}	0.3774	4.2×10^{-4}	0.3861
	3.6	99.57	4.4×10^{-5}	0.4328	5.0×10^{-4}	0.4353
	3.7	99.51	6.1×10^{-5}	0.4943	6.0×10^{-4}	0.4890
	3.8	99.44	8.2×10^{-5}	0.5623	7.1×10^{-4}	0.5474

study, two states with $I(J^P) = 1/2(1/2^-)$ and $I(J^P) = 1/2(3/2^-)$ are generated from the VB interactions. Determining which one can be considered as the $\Xi(2120)$ requires further investigation, especially concerning its strong decay width. This is mainly because the strong decay width heavily depends on the internal components of the hadron. Here, we find that if the $\Xi(2120)$ is a bound state with $I(J^P) = 1/2(1/2^-)$, it contains the dominant $\bar{K}^*\Sigma$ component and smaller but non-negligible $\bar{K}^*\Lambda$, $\rho\Xi$, and $\phi\Xi$ components. However, almost only the $\bar{K}^*\Sigma$ component contributes to the $\Xi(2120)$ if it is a VB bound state with $I(J^P) = 1/2(3/2^-)$. These comparisons are illustrated in Table V.

The individual contributions of the $\bar{K}^*\Sigma$, $\rho\Xi$, $\bar{K}^*\Lambda$, $\phi\Xi$, and $\omega\Xi$ channels for the bound states with $I(J^P) = 1/2(1/2^-)$ and $I(J^P) = 1/2(3/2^-)$ are calculated and presented in Fig. 2. It is found that the $\bar{K}^*\Sigma$, $\phi\Xi$, and $\bar{K}^*\Lambda$ single-channel interactions play a dominant role, while single-channel interactions of the $\rho\Xi$ and $\omega\Xi$ have no contribution for the bound state in the $I(J^P) = 1/2(1/2^-)$ case. However, for the bound state with $I(J^P) = 1/2(3/2^-)$, nearly all considered single-channel interactions give a contribution. By comparing with the

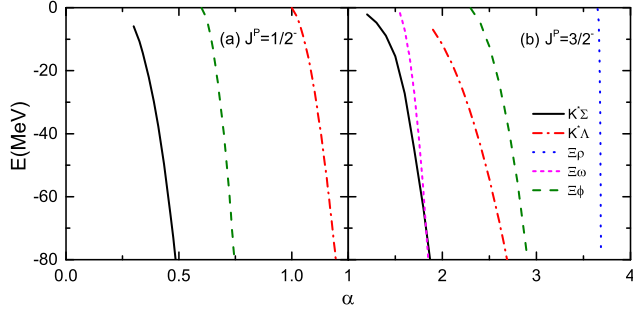


FIG. 2. The binding energy of bound states with different spin obtained from the single-channel interactions as the function of the cutoff α . The solid black line, dashed red line, dotted blue line, dash-dotted magenta line, and dash-dot-dotted olive line represent the bound states that appear in the $\bar{K}^*\Sigma$, $\bar{K}^*\Lambda$, $\rho\Xi$, $\omega\Xi$, and $\phi\Xi$ interactions, respectively.

results shown in Table V, we can observe that interference interactions among them are still significant. For better clarity, let us use the bound state in the $I(J^P) = 1/2(1/2^-)$ channel as an example. We find that interference interactions now lead to contributions from $\rho\Xi$ and $\omega\Xi$ to the bound state, whereas the pure $\rho\Xi$ and $\omega\Xi$ interactions made no contribution.

By comparing, we also find that the size of molecular components is inversely proportional to the parameter α in the $I(J^P) = 1/2(1/2^-)$ channel. That means the smaller the α , the larger the ratio of the corresponding molecular component to the total molecular component. You can find from Fig. 2 that the interaction contributions correspond to the smallest α for the $\bar{K}^*\Sigma$ channel, the intermediate α for the $\phi\Xi$ channel, and the largest α for the $\bar{K}^*\Lambda$. However, you can clearly see that the primary component of the molecule is $\bar{K}^*\Sigma$, followed by $\phi\Xi$, with $\bar{K}^*\Lambda$ being the smallest (see Table V). Similar conclusions cannot be obtained for other channels. Such as in the case of the $I(J^P) = 1/2(3/2^-)$ channel, you can find that the corresponding minimum α , but the dominant molecular component, remains the $\bar{K}^*\Sigma$ channel. However, the α corresponding to the $\phi\Xi$ channel, which ranks as the second major molecular component, is not the second smallest. A possible explanation for this is that the interference interaction among the channels in the case of $I(J^P) = 1/2(3/2^-)$ is stronger than that in the $I(J^P) = 1/2(1/2^-)$ channel. Moreover, the closer parameter α is to 1, the more it makes the corresponding component become the dominant component of the molecule. This is likely why people generally consider the results obtained with $\alpha \simeq 1$ in the one-boson exchange model to be the most reliable. Nevertheless, based on experimental information, people obtained a relatively wide range of variations for the parameter α [70–76], which encompasses the values considered in this work.

Now, we turn to discuss the possible high-wave molecular states related to the $\Xi(2030)$ through the VB

interactions, which have not been previously explored in other works, such as those referenced in Refs. [33,39,40]. The experimental analysis [34] favors a spin not less than $J = 5/2$ for the $\Xi(2030)$, which is also suggested by PDG [1]. As discussed above, the system with a spin-parity $J^P = 5/2^-$ and spin $J \geq 7/2$ is at least a D -wave state, whose contribution should be small. Indeed, we find that the bound state with $I(J^P) = 1/2(5/2^-)$ is not survived (see Table III). That means the $\Xi(2030)$ state cannot be accommodated in the current D -wave VB molecular picture. The only possible spin-parity to interpret the $\Xi(2030)$ in our molecular picture is $J^P = 5/2^+$, corresponding to the P/F -wave VB molecule (see Table III). Fortunately, a bound state with $J^P = 5/2^+$ can be found at a cutoff of about $\alpha = 3.4$ in our model, as expected, and with the increase of the cutoff, its mass can reach 2030 MeV. Notably, the study in Ref. [42] suggested that P -wave contributions are still considerable and may be observed in experiments.

In Table V, it is evident that the dominant contribution to the bound state with $J^P = 5/2^+$ primarily arises from the $\bar{K}^*\Sigma$ component, accounting for nearly 99.44% to 99.67% of the total component when α falls within the range of $\alpha = 3.4$ –3.8. It is important to note that the repulsive centrifugal force for the angular momentum (L) is the same in states with $J^P = 5/2^+$ and $J^P = 5/2^-$, as given by $L(L+1)/2\mu r^2$. However, we observe a bound state in the case of $J^P = 5/2^+$, while molecular formation is prohibited for $J^P = 5/2^-$. One possible explanation for this difference lies in the significant variation of meson-exchange forces between these two cases.

In addition to the molecule discussed earlier, we are also interested in exploring other possible bound states arising from the VB interaction. Table IV reveals the presence of a bound state with $J^P = 1/2^+$ occurring around $\alpha = 1.0$ –1.3 and another bound state with $J^P = 3/2^+$ forming at $\alpha = 2.7$ –3.0. Given the predominant contribution of low partial waves, it is expected that these two molecular states possess significant P -wave VB components (refer to Table III).

IV. SUMMARY

Inspired by the LHCb observation of the pentaquark states and their molecular interpretations, we have studied possible bound states from the $VB = (\bar{K}^*\Sigma/\rho\Xi/\bar{K}^*\Lambda/\phi\Xi/\omega\Xi)$ interaction by solving a Schrödinger equation within the one-boson exchange model. A bound state with the quantum number $I(J^P) = 1/2(5/2^+)$ from the VB interaction is produced at $\alpha = 3.4$. This bound state can be associated with the $\Xi(2030)$ as a P -wave molecular state. Four other bound states with quantum numbers $J^P = 1/2(1/2^-)$, $1/2(3/2^-)$, $1/2(1/2^+)$, and $1/2(3/2^+)$ are also produced from the $VB = (\bar{K}^*\Sigma/\rho\Xi/\bar{K}^*\Lambda/\phi\Xi/\omega\Xi)$ interaction.

For the $\Xi(2030)$, our study showed that it could be a P -wave VB bound state with spin-parity $J^P = 5/2^+$,

consistent with the available experimental information. On the other hand, we do not have enough experimental information to determine which bound state produced from the VB interaction is the $\Xi(2120)$. If we follow the assignment in Ref. [33] that the $\Xi(2120)$ is a molecular bound state with $J^P = 1/2(3/2^-)$, it is interesting to see that the $\Xi(2120)$ and $\Xi(2030)$ exhibit a pattern. It is worth noting that if $\Xi(2012)$ is an S -wave molecular state with $J^P = 3/2^-$, we suggest determining its spin and parity by studying its decay width, owing to the larger difference in their molecular components.

Clearly, more experimental efforts are needed to better understand the nature of the $\Xi(2120)$ and test the scenario proposed in the present study. There exist plans to study double-strangeness baryons at facilities such as JLab, JPARC, and PANDA. We strongly recommend that our experimental colleagues study the $\Xi(2030)$, the $\Xi(2120)$, and the other double strangeness baryons.

ACKNOWLEDGMENTS

This work was supported by the National Natural Science Foundation of China under Grant No. 12005177.

-
- [1] R. L. Workman *et al.* (Particle Data Group), *Prog. Theor. Exp. Phys.* **2022**, 083C01 (2022).
- [2] S. Godfrey and N. Isgur, *Phys. Rev. D* **32**, 189 (1985).
- [3] S. Capstick and N. Isgur, *Phys. Rev. D* **34**, 2809 (1986).
- [4] E. Oset and A. Ramos, *Nucl. Phys.* **A635**, 99 (1998).
- [5] J. A. Oller and U. G. Meißner, *Phys. Lett. B* **500**, 263 (2001).
- [6] Y. Nemoto, N. Nakajima, H. Matsufuru, and H. Suganuma, *Phys. Rev. D* **68**, 094505 (2003).
- [7] J. M. M. Hall, W. Kamleh, D. B. Leinweber, B. J. Menadue, B. J. Owen, A. W. Thomas, and R. D. Young, *Phys. Rev. Lett.* **114**, 132002 (2015).
- [8] M. Ablikim *et al.* (BESIII Collaboration), *Phys. Rev. Lett.* **110**, 252001 (2013).
- [9] Z. Q. Liu *et al.* (Belle Collaboration), *Phys. Rev. Lett.* **110**, 252002 (2013); **111**, 019901(E) (2013).
- [10] Q. Wang, C. Hanhart, and Q. Zhao, *Phys. Rev. Lett.* **111**, 132003 (2013).
- [11] J. He, *Phys. Rev. D* **90**, 076008 (2014).
- [12] E. Wilbrink, H. W. Hammer, and U. G. Meißner, *Phys. Lett. B* **726**, 326 (2013).
- [13] R. Aaij *et al.* (LHCb Collaboration), *Phys. Rev. Lett.* **122**, 222001 (2019).
- [14] H. X. Chen, W. Chen, and S. L. Zhu, *Phys. Rev. D* **100**, 051501 (2019).
- [15] F. K. Guo, H. J. Jing, U. G. Meißner, and S. Sakai, *Phys. Rev. D* **99**, 091501 (2019).
- [16] C. W. Xiao, J. Nieves, and E. Oset, *Phys. Rev. D* **100**, 014021 (2019).
- [17] J. He, *Eur. Phys. J. C* **79**, 393 (2019).
- [18] C. J. Xiao, Y. Huang, Y. B. Dong, L. S. Geng, and D. Y. Chen, *Phys. Rev. D* **100**, 014022 (2019).
- [19] R. Aaij *et al.* (LHCb Collaboration), *Sci. Bull.* **66**, 1278 (2021).
- [20] T. Gutsche and V. E. Lyubovitskij, *Phys. Rev. D* **100**, 094031 (2019).
- [21] H. X. Chen, W. Chen, X. Liu, and X. H. Liu, *Eur. Phys. J. C* **81**, 409 (2021).
- [22] F. Z. Peng, M. J. Yan, M. Sánchez Sánchez, and M. P. Valderrama, *Eur. Phys. J. C* **81**, 666 (2021).
- [23] Z. G. Wang, *Int. J. Mod. Phys. A* **36**, 2150071 (2021).
- [24] R. Chen, *Phys. Rev. D* **103**, 054007 (2021).
- [25] F. Yang, Y. Huang, and H. Q. Zhu, *Sci. China Phys. Mech. Astron.* **64**, 121011 (2021).
- [26] F. K. Guo, C. Hanhart, U. G. Meißner, Q. Wang, Q. Zhao, and B. S. Zou, *Rev. Mod. Phys.* **90**, 015004 (2018).
- [27] T. Sekihara, *Prog. Theor. Exp. Phys.* **2015**, 091D01 (2015).
- [28] E. E. Kolomeitsev and M. F. M. Lutz, *Phys. Lett. B* **585**, 243 (2004).
- [29] S. Sarkar, E. Oset, and M. J. Vicente Vacas, *Nucl. Phys.* **A750**, 294 (2005); **A780**, 90(E) (2006).
- [30] K. T. Chao, N. Isgur, and G. Karl, *Phys. Rev. D* **23**, 155 (1981).
- [31] M. Pervin and W. Roberts, *Phys. Rev. C* **77**, 025202 (2008).
- [32] L. Y. Xiao and X. H. Zhong, *Phys. Rev. D* **87**, 094002 (2013).
- [33] K. P. Khemchandani, A. Martínez Torres, A. Hosaka, H. Nagahiro, F. S. Navarra, and M. Nielsen, *Phys. Rev. D* **97**, 034005 (2018).
- [34] R. J. Hemingway *et al.* (Amsterdam-CERN-Nijmegen-Oxford Collaboration), *Phys. Lett.* **68B**, 197 (1977).
- [35] N. P. Samios, M. Goldberg, and B. T. Meadows, *Rev. Mod. Phys.* **46**, 49 (1974).
- [36] M. Pavon Valderrama, J. J. Xie, and J. Nieves, *Phys. Rev. D* **85**, 017502 (2012).
- [37] J. B. Gay *et al.* (Amsterdam-CERN-Nijmegen-Oxford Collaboration), *Phys. Lett.* **62B**, 477 (1976).
- [38] A. P. Vorobev *et al.* (French-Soviet and CERN-Soviet Collaboration), *Nucl. Phys.* **B158**, 253 (1979).
- [39] E. Oset and A. Ramos, *Eur. Phys. J. A* **44**, 445 (2010).
- [40] D. Gamermann, C. Garcia-Recio, J. Nieves, and L. L. Salcedo, *Phys. Rev. D* **84**, 056017 (2011).
- [41] X. W. Kang and J. A. Oller, *Phys. Rev. D* **94**, 054010 (2016).
- [42] J. He, *Phys. Rev. D* **95**, 074004 (2017).
- [43] H. Q. Zhu and Y. Huang, *Phys. Rev. D* **105**, 056011 (2022).
- [44] Z. Y. Jian, H. Q. Zhu, F. Yang, Q. H. Chen, and Y. Huang, *Eur. Phys. J. A* **59**, 262 (2023).
- [45] R. Machleidt, K. Holinde, and C. Elster, *Phys. Rep.* **149**, 1 (1987).
- [46] R. Chen, X. Liu, X. Q. Li, and S. L. Zhu, *Phys. Rev. Lett.* **115**, 132002 (2015).

- [47] R. Chen and X. Liu, *Phys. Rev. D* **94**, 034006 (2016).
- [48] F. L. Wang, R. Chen, Z. W. Liu, and X. Liu, *Phys. Rev. C* **101**, 025201 (2020).
- [49] F. L. Wang, R. Chen, and X. Liu, *Phys. Rev. D* **103**, 034014 (2021).
- [50] N. Li and S. L. Zhu, *Phys. Rev. D* **86**, 074022 (2012).
- [51] Z. F. Sun, J. He, X. Liu, Z. G. Luo, and S. L. Zhu, *Phys. Rev. D* **84**, 054002 (2011).
- [52] B. Kubis and U. G. Meissner, *Nucl. Phys. A* **679**, 698 (2001).
- [53] K. P. Khemchandani, A. Martínez Torres, and J. A. Oller, *Phys. Rev. C* **100**, 015208 (2019).
- [54] E. E. Jenkins, M. E. Luke, A. V. Manohar, and M. J. Savage, *Phys. Lett. B* **302**, 482 (1993); **388**, 866(E) (1996).
- [55] D. Jido, A. Hosaka, J. C. Nacher, E. Oset, and A. Ramos, *Phys. Rev. C* **66**, 025203 (2002).
- [56] M. Bando, T. Kugo, S. Uehara, K. Yamawaki, and T. Yanagida, *Phys. Rev. Lett.* **54**, 1215 (1985).
- [57] M. Bando, T. Kugo, and K. Yamawaki, *Phys. Rep.* **164**, 217 (1988).
- [58] E. Oset, J. R. Pelaez, and L. Roca, *Phys. Rev. D* **67**, 073013 (2003).
- [59] P. Gonzalez, E. Oset, and J. Vijande, *Phys. Rev. C* **79**, 025209 (2009).
- [60] A. Bramon, A. Grau, and G. Pancheri, *Phys. Lett. B* **283**, 416 (1992).
- [61] G. Ecker, J. Gasser, A. Pich, and E. de Rafael, *Nucl. Phys. B* **321**, 311 (1989).
- [62] E. J. Garzon and E. Oset, *Eur. Phys. J. A* **48**, 5 (2012).
- [63] K. Chen, R. Chen, Z. F. Sun, and X. Liu, *Phys. Rev. D* **100**, 074006 (2019).
- [64] B. Kubis and U. G. Meissner, *Eur. Phys. J. C* **18**, 747 (2001).
- [65] F. E. Close and R. G. Roberts, *Phys. Lett. B* **316**, 165 (1993).
- [66] S. Y. Hsueh, D. Muller, J. Tang, R. Winston, G. Zapalac, E. C. Swallow, J. P. Berge, A. E. Brenner, P. S. Cooper, P. Grafstrom *et al.*, *Phys. Rev. D* **38**, 2056 (1988).
- [67] G. Breit, *Phys. Rev.* **34**, 553 (1929).
- [68] G. Breit, *Phys. Rev.* **36**, 383 (1930).
- [69] E. Hiyama, Y. Kino, and M. Kamimura, *Prog. Part. Nucl. Phys.* **51**, 223 (2003).
- [70] Y. Dong, A. Faessler, T. Gutsche, Q. Lü, and V. E. Lyubovitskij, *Phys. Rev. D* **96**, 074027 (2017).
- [71] D. Y. Chen, X. Liu, and T. Matsuki, *Phys. Rev. D* **87**, 054006 (2013).
- [72] H. Xu, J. J. Xie, and X. Liu, *Eur. Phys. J. C* **76**, 192 (2016).
- [73] X. Liu, B. Zhang, and S. L. Zhu, *Phys. Lett. B* **645**, 185 (2007).
- [74] P. Colangelo, F. De Fazio, and T. N. Pham, *Phys. Lett. B* **542**, 71 (2002).
- [75] C. Meng and K. T. Chao, *Phys. Rev. D* **75**, 114002 (2007).
- [76] X. Liu, Z. T. Wei, and X. Q. Li, *Eur. Phys. J. C* **59**, 683 (2009).